

**Selective readout and back-action reduction for wideband acoustic gravitational wave detectors**Michele Bonaldi,<sup>1,\*</sup> Massimo Cerdonio,<sup>2</sup> Livia Conti,<sup>2</sup> Michel Pinard,<sup>3</sup> Giovanni A. Prodi,<sup>4</sup> Luca Taffarello,<sup>5</sup> and Jean Pierre Zendri<sup>5</sup><sup>1</sup>*Istituto di Fotonica e Nanotecnologie CNR-ITC and INFN Trento, I-38050 Povo (Trento), Italy*<sup>2</sup>*INFN Padova Section and Department of Physics, University of Padova, via Marzolo 8, I-35100 Padova, Italy*<sup>3</sup>*Laboratoire Kastler Brossel, 4 place Jussieu, F75252 Paris, France*<sup>4</sup>*Department of Physics, University of Trento and INFN Trento, I-38050 Povo (Trento), Italy*<sup>5</sup>*INFN Padova Section, via Marzolo 8, I-35100 Padova, Italy*

(Received 22 December 2002; published 25 November 2003)

We present the concept of the “selective readout” for the recently proposed dual detector [M. Cerdonio *et al.*, Phys. Rev. Lett. **87**, 031101 (2001)] of gravitational waves which is a sensitive and broadband resonant-mass detector. The advantage of the proposed detection scheme is that it is made sensitive only to the acoustic modes of the masses forming the detector that have quadrupolar symmetry, and thus carry the signal, while it rejects efficiently the noise contribution from the other modes, either of thermal or back-action origin. The total effect is that the sensitivity of a dual detector equipped with the selective readout is flat within a wide frequency range and can be as good as  $\sim 8 \times 10^{-24} / \sqrt{\text{Hz}}$  between 1.3 and 4 kHz for a silicon carbide detector, 3 m in diameter.

DOI: 10.1103/PhysRevD.68.102004

PACS number(s): 04.80.Nn, 95.55.Ym

**I. INTRODUCTION**

Substantial progress has been made over the last 40 years in preparing instruments and methods to search for gravitational waves (GW) from the cosmos [1]. Five bar detectors distributed worldwide have recently operated for a few years as a network, setting significant upper limits to the rate of violent GW burst events impinging on Earth from the Galaxy [2,3]. The first generation of long base line interferometric detectors [4,5] are now starting their operation and are giving results from the first science runs [6].

The performance of traditional acoustic detectors, bars, suffers from two main limits: one comes from the cross section to the GW signal, which sets the peak sensitivity, and one comes from the limited frequency range of high sensitivity. In order to efficiently couple the signal amplitude to the final readout [7], all bar detectors employ a resonant transducer, i.e., a secondary oscillator attached to the bar and tuned to it. The main drawback is that the useful bandwidth becomes intrinsically limited, up to typically 10% of the resonant frequency of the main resonator (i.e., the bar). Moreover, the coupling of a second oscillator to the bar has proved so far to lower the mechanical quality factor of the main resonator, thus reducing its potential sensitivity. Advanced versions of the traditional acoustic detectors are spherical resonant detectors [8–10], now being built by several groups worldwide [11–13]; while gaining in peak sensitivity, they do not solve the bandwidth problem, as they still employ resonant transducers.

Some of us have recently proposed a different strategy that takes care of both the sensitivity and the bandwidth limit of the acoustic detectors. This is the “dual” detector [14]: a

dual detector is formed by two nested massive bodies whose quadrupolar modes (i.e., the modes sensitive to the GW signal) resonate at different frequencies. In Ref. [14] the two resonators are two spheres, an inner full one and a hollow outer one. In a dual detector the signal is read in the gap between the two masses as their differential deformations: the centers of mass of the two bodies coincide and remain mutually at rest while the masses resonate, thus providing for the rest frame of the measurement. The sensitivity of the dual detector is predicted to be of interest in the frequency range between the first quadrupolar modes of the two masses. This can be as broad as a few kilohertz in the kilohertz range, thus covering the frequency band where GW signals from fully relativistic stellar sources are expected [15].

In this paper we describe a detection scheme specifically designed for the dual detector and which we call selective readout. This readout is designed to be sensitive only to the acoustic modes of the masses forming the detector that have quadrupolar symmetry, and thus are excited by the GW signal. At the same time, the readout rejects efficiently the contribution from the other modes, either of thermal or back-action origin. The overall effect is a significant enhancement in the sensitivity.

In Sec. II we will discuss the principle of operation of a dual detector made by two cylindrical nested masses equipped by a selective readout. We illustrate at first the simple case of a dual system with only two mechanical resonances (Sec. II A); then we consider the full modal expansion for the system and introduce the selective readout concept (Sec. II B); in the end we give a readout weight function selective for the GW detection and derive the system transfer function (Sec. II C). In Sec. III we show the expected sensitivity at the standard quantum limit of two specific detector configurations. Finally, in Sec. IV we discuss some issues about the required readout performances and we compare the dual detector with advanced long base line interferometers.

\*Corresponding author. Electronic address: bonaldi@science.unitn.it

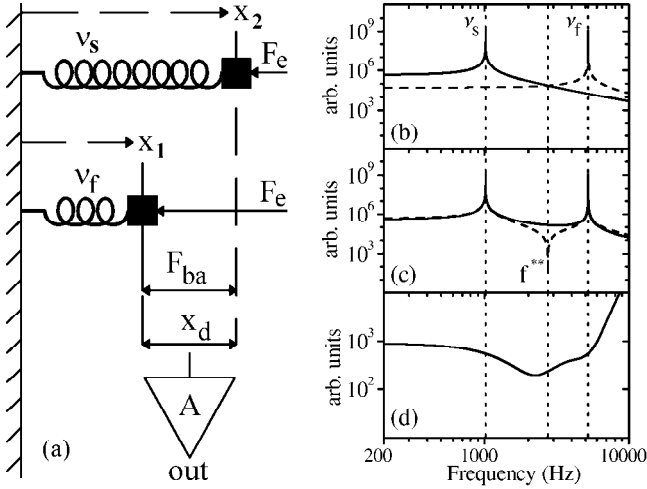


FIG. 1. (a) One-dimensional “dual” detector: the same force  $F_e$  is measured by the relative displacement  $x_d$  of two resonators. (b) Transfer functions of the slow resonator (continuous line) and of the fast resonator (dashed line). (c) Dual detector transfer functions: signal  $H_{F_e} = x_d/F_e$  (continuous line), back action  $H_{ba} = x_d/F_{ba}$  (dashed line). (d) Wideband optimized noise.

## II. DUAL DETECTORS

### A. One-dimensional model: Standard quantum limit and back-action reduction

A basic dual detector can be represented as the simple one-dimensional system shown in Fig. 1(a) formed by two different and independent mechanical oscillators whose positions are  $x_1$  and  $x_2$ ; a force  $F_e$  driving the two oscillators is evaluated by measuring the difference  $x_d = x_1 - x_2$ . In the frequency region between the resonant frequencies of the two oscillators,  $F_e$  drives the slow resonator above its resonance  $\nu_s$  and the fast one below its resonance  $\nu_f$ . The responses of the two are thus out of phase by  $\pi$  radians and therefore the differential motion  $x_d$  results in a signal enhancement with respect to the response of the single oscillator [Fig. 1(b)], as shown by the transfer function  $H_{F_e} = x_d/F_e$  [Fig. 1(c)].

In addition such a scheme leads to a reduction of the back-action noise within the frequency range of sensitivity of the detector. In fact the back-action noise force drives coherently the two oscillators in *opposite* directions: the system response is nearly exactly in phase and the consequent differential displacement is highly depressed at a frequency  $f^{**}$ , as shown in the transfer function  $H_{ba} = x_d/F_{ba}$  [Fig. 1(c)]. The features of the back-action reduction are discussed in more details in Ref. [16].

We measure  $x_d$  with a real displacement amplifier, described as an ideal amplifier with an additive displacement noise generator and force noise generator that back acts on the system under measurement. Let  $S_{XX}(\omega) = S_{xx}$  and  $S_{FF}(\omega) = S_{ff}$  be, respectively, the frequency-independent power spectral densities of these noise generators. The total displacement noise due to the amplifier is then  $S_{xx} + |H_{ba}(\omega)|^2 S_{ff}$  and the noise power spectrum on the measurement of  $F_e$  is (see, for instance, Ref. [17])

$$S_{F_e}(\omega) = [S_{xx} + |H_{ba}(\omega)|^2 S_{ff}] / |H_{F_e}(\omega)|^2. \quad (1)$$

If we take as reference an operation at the standard quantum limit (SQL), we may consider  $S_{xx} S_{ff} = \hbar^2$ , and the noise figure can be optimized by adjusting the ratio  $S_{xx}/S_{ff}$ . In a wide bandwidth detection strategy  $S_{xx}$  and  $S_{ff}$  must be balanced to give the lowest noise within the bandwidth. In doing so we profit by the subtraction effect in the back-action noise transfer function  $H_{ba}$ , and obtain a dip at the frequency  $f^{**}$ , as shown in Fig. 1(d). We finally notice that, to fully exploit the back-action reduction features,  $f^{**}$  should be placed, by a proper choice of the system parameters, amid the oscillator frequencies.

### B. Full modal expansion and selective readout

In the case of a three-dimensional body, the dynamics of elastic deformations is given as the superposition of the dynamics of an almost infinite number of normal modes of vibration [18]. An obvious way to preserve the convenient features for signal and back-action noise outlined above is to bring the real system to be as close as possible to the idealized two-mode system. In fact when only the first quadrupolar mode can be considered for each body, the response to a GW of such a system can again be described by the simple one-dimensional model. This can be accomplished with the novel selective readout we propose here, capable of rejecting a large number of normal modes on the basis of their symmetry. This *geometrically based mode selection* senses the surface position of a body on specific regions, so that the related deformations can be combined with a weight/sign properly chosen to optimize the total response to normal modes of quadrupolar symmetry.

Such a strategy to select specific vibrational modes and to reject a class of unwanted modes is conceptually different from the strategy now employed in GW acoustic detectors. Resonant bar detectors [2,3] and spherical detectors [8–10] reconstruct the amplitude of the normal modes excited by the GW by the use of resonant displacement readouts coupled to the modes. With a proper choice of the readout surfaces, the resonant scheme is not sensitive to the thermal noise of out of resonance modes and gives an efficient frequency based mode selection. However this feature necessarily limits the detector bandwidth, due to the thermal noise contribution of the resonant transducer, as mentioned above. By contrast the geometrically based mode selection selects gravitationally sensitive normal modes by means of their geometrical characteristics, and shows a significant rejection of nonquadrupolar modes without affecting the detector bandwidth. For this reason it can be effectively applied to a dual wideband detector.

Without loss of generality, we apply these new concepts to a dual cylinder detector [Fig. 2(a)], a convenient geometry where the advantages of the proposed scheme can be fully exploited. In the dual cylinder we average the differential displacement in four distinct areas  $x_1, \dots, x_4$  [Fig. 2(b)] and combine them to obtain  $X_d = x_1 + x_3 - x_2 - x_4$ . The detector displays its maximal sensitivity when the GW propagates

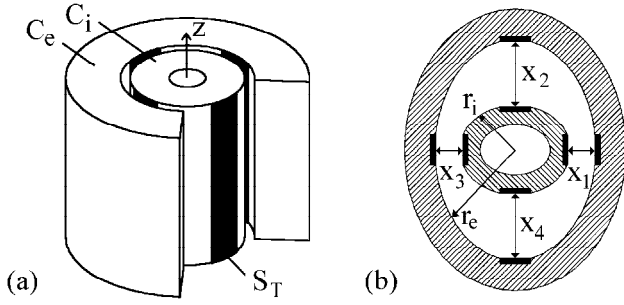


FIG. 2. (a) The two concentric cylinders  $C_e$ ,  $C_i$  are made of materials of density  $\rho_e$ ,  $\rho_i$  and have the same height. The inner cylinder may also have null internal radius. The relative distance between the two bodies is measured in four regions (in black), each of area  $S_T$ , for the whole cylinder height. (b) Section of the detector showing the signal enhancement obtained when a GW signal drives the external cylinder above resonance and the internal cylinder below resonance. The difference  $X_d = x_1 + x_3 - x_2 - x_4$ , proportional to the GW strength, is not dependent on a number of non-GW sensitive modes.

along the  $z$  axis, the symmetry axis of the system. The corresponding force does not depend on  $z$  and the system response can be well described by plane strain solutions, where the displacements are functions of  $x$  and  $y$  only and the displacement along  $z$  vanishes. All the components of the internal stress are also independent of  $z$ . In this case the displacement normal modes of a single cylinder, eigenfunctions of the free body dynamic equations, are functions of the kind [19]

$$\mathbf{w}_{a,n}^+(\mathbf{r}) = f_{a,n} \cos(a\theta) \mathbf{i}_r + g_{a,n} \sin(a\theta) \mathbf{i}_\theta,$$

$$\mathbf{w}_{a,n}^\times(\mathbf{r}) = -f_{a,n} \sin(a\theta) \mathbf{i}_r + g_{a,n} \cos(a\theta) \mathbf{i}_\theta,$$

where the functions  $f_{a,n}$ ,  $g_{a,n}$  are linear combinations of Bessel functions of the coordinate  $r$ , with coefficients given by the boundary conditions. The integer  $a$  represents the angular symmetry of the mode, while  $n$  identifies the mode order within the angular family. The orthogonal displacement fields  $\mathbf{w}_{a,n}^+$ ,  $\mathbf{w}_{a,n}^\times$  represent the same radial distribution of the deformation, mutually rotated by  $\pi/2a$ : for this reason they share the same eigenvalue  $\omega_{a,n}$ , called resonant frequency of the mode. Any displacement  $\mathbf{u}$  may be written as linear superposition of these basis functions:

$$\mathbf{u}(\mathbf{r}, t) = \sum_{s,a,n} \mathbf{w}_{a,n}^s(\mathbf{r}) q_{a,n}^s(t), \quad (2)$$

where the time dependent coefficients are determined by the force acting on the body and  $s = +, \times$ .

### C. Weight function and mechanical transfer functions

A  $+$  polarized GW propagating along the  $z$  axis applies the force density  $F_{gw}(t) \mathbf{G}_{gw}(\mathbf{r})$  on the mass of density  $\rho$ :

$$F_{gw}(t) = \frac{1}{2} \rho \ddot{h}(t),$$

$$\mathbf{G}_{gw}(\mathbf{r}) = r \cos(2\theta) \mathbf{i}_r - r \sin(2\theta) \mathbf{i}_\theta. \quad (3)$$

For symmetry reasons this force can only excite  $\mathbf{w}^+$  quadrupolar ( $a=2$ ) modes. A “weight function” approach to the problem will give the mathematical framework to study the selective readout, which implements the difference  $X_d = x_1 + x_3 - x_2 - x_4$  [Fig. 2(b)]. If  $\mathbf{u}_e$  and  $\mathbf{u}_i$  are the displacements of the cylinder  $C_e$  and  $C_i$  [20], we define the observable physical quantity of the system as

$$X_d(t) = \int [\mathbf{u}_e(\mathbf{r}, t) + \mathbf{u}_i(\mathbf{r}, t)] \cdot \frac{\mathbf{P}_4(\mathbf{r})}{P_N} dV, \quad (4)$$

where the “selective” measurement strategy and detection scheme is implemented by the weight function  $\mathbf{P}_4(\mathbf{r}) = P_4^r(r) P_4^\theta(\theta) \mathbf{i}_r$ , where

$$P_4^r = \delta(r - r_e) - \delta(r - r_i),$$

$$P_4^\theta = \sum_{m=0}^1 \sum_{n=0}^4 (-1)^{n+m} \Theta \left[ \theta + (-1)^m \alpha - n \frac{\pi}{2} \right], \quad (5)$$

and  $\Theta(x)$  represents the unit step function. The normalization is  $P_N = S_T$ , area of one sampling region [Fig. 2(a)]. Here the term  $P_4^r$  gives the requested displacement difference  $r_e - r_i$  [Fig. 2(b)], while  $P_4^\theta$  reduces the angular integral over four distinct regions,  $2\alpha$  wide, centered around  $\theta = 0, \pi/2, \pi, 3\pi/2$  [Fig. 4(a)]. A value  $\alpha = 0.3$  rad is assumed to perform the following calculations. For comparison we consider a nonselective readout system, which senses the displacement over a single area, centered, for example, at  $\theta = 0$ . Its weight function  $\mathbf{P}_1$  has angular component  $P_1^\theta = \Theta(\theta + \alpha) - \Theta(\theta - \alpha) + \Theta(\theta + \alpha - 2\pi) - \Theta(\theta - \alpha - 2\pi)$ , while the radial dependence and the normalization remain the same as  $\mathbf{P}_4$ .

A practical readout configuration implementing the selective readout scheme  $\mathbf{P}_4$  is a series of four capacitive transducers (Fig. 3). The transducers are gradiometrically connected to obtain the quadrupolar modes sensitivity. Notice that to obtain the back-action reduction the readout must be necessarily sensed by a single superconducting quantum interference device (SQUID) amplifier. The nonselective readout scheme  $\mathbf{P}_1$  may be implemented by a single capacitive transducer configuration measuring the distance  $x_1$ .

When we evaluate the observable, Eq. (4), by using the expansion, Eq. (2), and the weight functions  $\mathbf{P}_4$  or  $\mathbf{P}_1$ , each  $\mathbf{w}_{a,n}^+$  mode contribution depends on its angular symmetry  $a$ . As shown in Fig. 4(b), in both cases the modes contribution oscillates and rapidly decreases, due to the averaging over the area  $S_T$ . But in the case of  $\mathbf{P}_4$  only the symmetry values  $a = 2 + 4k$ , with  $k$  non-negative integer, give non-null contributions to our observable, Eq. (4). To summarize, the quadrupolar modes family ( $k=0$ ) contribution is essentially pre-

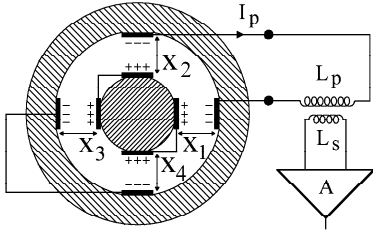


FIG. 3. Schematic cross section of a dual cylinder equipped with a selective capacitive readout. Four identical capacitors are charged with a constant charge and connected as shown; the circulating current  $I_p$  is proportional to the variations of  $X_d = x_1 + x_3 - x_2 - x_4$ . The current is then coupled to the SQUID amplifier  $A$  by a flux transformer made by the coils  $L_p$  and  $L_s$ . The auxiliary electronic circuitry necessary to obtain the proper constant charge distribution is not shown; in particular decoupling capacitors must be used to prevent the capacitors from discharging.

served, many mode families are rejected ( $a \neq 2 + 4k$ ,  $k \geq 0$ ) and the residual higher-order families ( $a = 2 + 4k$ ,  $k > 0$ ) give a reduced contribution.

We point out that the normal modes  $\mathbf{w}^\times$ , proportional to  $\sin(a\theta)$  and excited by  $\times$ -polarized gravitational waves, are rejected by  $\mathbf{P}_4(\mathbf{r})$  for every value of  $a$ . When a second readout system, identical but rotated by  $\pi/4$ , is employed to detect these  $\mathbf{w}^\times$  modes, any  $z$  axis propagating GW can be fully characterized in terms of intensity and polarization.

The system behavior is fully described by the transfer function  $T_{X_d} \equiv \tilde{X}_d(\omega)/\tilde{F}(\omega)$ , which gives the observable  $X_d$  induced by a generic driving force density  $F(t)\mathbf{G}(\mathbf{r})$  [21]. We call  $(\mathbf{w}_{a,n}^s, \omega_{a,n})$  and  $(\mathbf{v}_{a,n}^s, \varpi_{a,n})$  the normal modes and eigenfrequencies of the cylinder  $C_e$  and  $C_i$ , while the loss

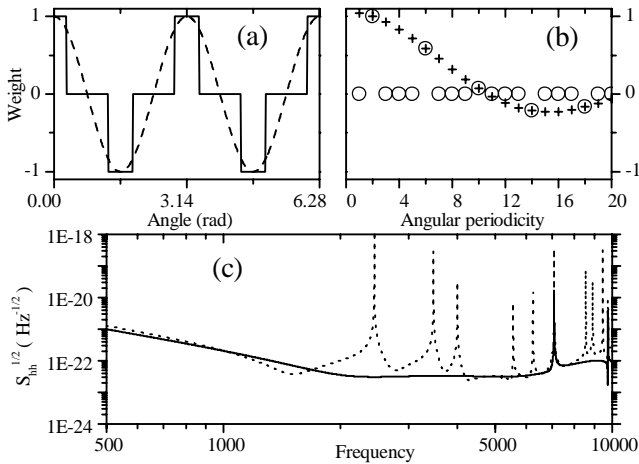


FIG. 4. (a) Angular dependence of the weight function  $\mathbf{P}_4$  (continuous line) and of the displacement induced by a  $\mathbf{w}^+$  mode (dashed line) with symmetry  $a=2$ ; the mode contribution is proportional to the integral of the product of these two functions. (b) Normalized angular contribution of normal modes as a function of  $a$  evaluated for the weight functions  $\mathbf{P}_4$  (hollow symbols) and  $\mathbf{P}_1$  (crosses). (c) Predicted sensitivity of a Mo dual cylinder detector (same as Fig. 5) with the selective readout  $\mathbf{P}_4$  (continuous line) and with the standard readout  $\mathbf{P}_1$  (dotted line).

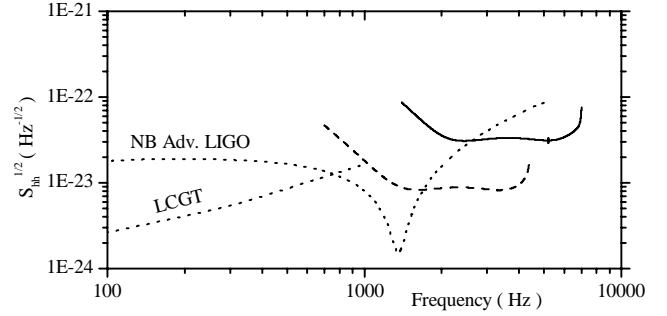


FIG. 5. Predicted spectral strain SQL sensitivities of two different dual detector configurations. The predicted SQL sensitivities of two advanced interferometric detectors are also shown (dotted lines): LCGT and a narrow band design of Advanced LIGO. Continuous line: Mo dual detector, inner cylinder radius 0.25 m, outer cylinder internal-external radius 0.26–0.47 m, height 2.35 m, weight 4.8+11.6 tons, fundamental quadrupolar modes 1012 Hz and 5189 Hz, amplifier noise  $S_{xx} = 10 \times 10^{-46} \text{ m}^2/\text{Hz}$ ,  $Q/T > 2 \times 10^8 \text{ K}^{-1}$ . Dashed line: SiC detector, inner cylinder radius 0.82 m, outer cylinder internal-external radius 0.83–1.44 m, height 3 m, weight 20.5–41.7 tons,  $S_{xx} = 6 \times 10^{-46} \text{ m}^2/\text{Hz}$ ,  $Q/T > 2 \times 10^8 \text{ K}^{-1}$ .

angles  $(\phi, \psi)$ , inversely proportional to the mode quality factor  $Q$ , describe the dissipation. We have

$$T_{X_d}(\omega) = \sum_{s,a,n} \frac{\int \mathbf{G}(\mathbf{r}) \cdot \mathbf{w}_{a,n}^s(\mathbf{r}) dV \int \mathbf{w}_{a,n}^s(\mathbf{r}) \cdot \frac{\mathbf{P}(\mathbf{r})}{P_N} dV}{\rho_e [(\omega_{a,n}^2 - \omega^2) + i\omega_{a,n}^2 \phi_{a,n}(\omega)]} + \frac{\int \mathbf{G}(\mathbf{r}) \cdot \mathbf{v}_{a,n}^s(\mathbf{r}) dV \int \mathbf{v}_{a,n}^s(\mathbf{r}) \cdot \frac{\mathbf{P}(\mathbf{r})}{P_N} dV}{\rho_i [(\varpi_{a,n}^2 - \omega^2) + i\varpi_{a,n}^2 \psi_{a,n}(\omega)]}, \quad (6)$$

where  $\mathbf{P}(\mathbf{r})$  can be  $\mathbf{P}_4(\mathbf{r})$  or  $\mathbf{P}_1(\mathbf{r})$ . If  $F(t)$  and  $\mathbf{G}(\mathbf{r})$  are given by Eq. (3), by Eq. (6) we calculate the system transfer function to a GW, defined as  $H_{g_w}(\omega) \equiv \tilde{X}_d(\omega)/\tilde{h}(\omega)$ . In the simple case  $\rho_e = \rho_i = \rho$ , we have

$$H_{g_w}(\omega) = -(\rho\omega^2/2)T_{X_d}(\omega)|_{\mathbf{G}(\mathbf{r})=\mathbf{G}_{g_w}(\mathbf{r})}, \quad (7)$$

while the more general case is straightforward. The readout back-action force is applied in the sensing areas with the same intensity but opposite sign for the two bodies, so that its spatial density is given by  $\mathbf{P}(\mathbf{r})/P_N$ . The corresponding system transfer function is then

$$H_{ba}(\omega) \equiv T_{X_d}(\omega)|_{\mathbf{G}(\mathbf{r})=\mathbf{P}(\mathbf{r})/P_N}, \quad (8)$$

### III. DETECTOR SENSITIVITY

In close analogy with Eq. (1), the transfer functions, Eqs. (7) and (8), give the detector sensitivity to GW as

$$S_{hh}(\omega) = [S_{xx} + |H_{ba}(\omega)|^2 S_{ff}] / |H_{g_w}(\omega)|^2. \quad (9)$$

As discussed above,  $S_{xx}$  and  $S_{ff}$  are the frequency-independent power spectral densities that define the amplifier

noise performances. For operation at the SQL we consider  $S_{xx}S_{ff}=\hbar^2$  and optimize the noise figure by adjusting the ratio  $S_{xx}/S_{ff}$ .

In Fig. 4(c) we compare the sensitivities of a detector, evaluated for the selective readout  $\mathbf{P}_4$  and for the single area readout  $\mathbf{P}_1$ . The main effect of the selective readout is to cancel out both thermal and back-action noise contributions due to the nonquadrupolar modes, so that a flat response is obtained in the full bandwidth of few kilohertz and the back-action reduction feature is exploited. We also notice that the use of large readout sensing area highly reduces the thermal noise due to the cumulative effect of all the normal modes [22]. In fact, as the shorter wavelength modes are averaged out, a very good transfer function convergence may be obtained by adding less than 100 modes.

Finite element analysis demonstrates the selective readout rejection capabilities also for many classes of three-dimensional vibrational modes. The sensitivity enhancement over the standard readout scheme is then not limited to our plane strain approximation, and the dual cylinder configuration could be evolved in a complete detector.

To show the limits of our design, we evaluate the sensitivity at the SQL of some practical configurations of detector material and geometry. As usual a low dissipation material is required to reduce the effect of the thermal noise. Molybdenum represents an interesting choice, as it shows high cross section for GW and its mechanical dissipation was investigated at low temperature giving  $Q/T > 2 \times 10^8 \text{ K}^{-1}$  for acoustic normal modes [23]. In Figs. 4 and 5 the SQL sensitivity of a Mo detector with dimensions within the present technological production capabilities is shown. In Fig. 5 we also show the SQL of a detector made of SiC, a ceramic material currently used to produce large mirrors or structures [24], with mechanical and thermal properties of interest here but not yet characterized in terms of low temperature mechanical dissipation.

#### IV. DISCUSSION AND CONCLUSION

The dual cylinder sensitivity curves are obtained by using a quantum limited readout with displacement sensitivity of

the order of  $3 \times 10^{-23} \text{ m}/\sqrt{\text{Hz}}$ . This figure is impressive and indeed has not been achieved so far. The assessment of the feasibility of such sensitivity is currently object of an R&D program and a detailed technological discussion goes beyond the scope of the present paper. Here we will address only a few general issues.

The lowest achieved experimental displacement noise we have achieved is about  $5 \times 10^{-20} \text{ m}/\sqrt{\text{Hz}}$  [25,26] in the kilohertz range. This has been demonstrated by two different kinds of readout which we are developing: the capacitive one [27] employing a dc-SQUID amplifier and the optical one [28] based on Fabry-Perot resonators. Both readouts can show significant improvements in the near future, so to reach sensitivities of a few  $10^{-22} \text{ m}/\sqrt{\text{Hz}}$ . For the capacitive readout, better dc-SQUID amplifiers are becoming available with sensitivities much closer to the quantum limit [29]. In addition, the efficiency of the transducer can be improved by increasing the bias electric field: a value of the breakdown field of the order of  $3 \times 10^8 \text{ V/m}$  has been reported in recent literature [30]. For the optical readout, the improvement relies on the increase of the finesse to  $10^6$  [31], of the input power up to few watts, and of the measurement area up to few  $\text{cm}^2$  [32].

To achieve the  $10^{-23} \text{ m}/\sqrt{\text{Hz}}$  displacement sensitivity range, nonresonant mechanical amplification of the detector deformations [33] could be implemented. Mechanical amplifiers based on the elastic deformation of monolithic devices (compliant mechanisms) are well known for their applications in mechanical engineering [34]. Their application to GW detectors seems promising but the contributed noise needs to be investigated thoroughly.

We believe that the potential sensitivity of the dual detector is of utmost interest. In fact the selective readout scheme applied to the dual concept allows the design of detectors tailored for relatively high frequency GW and showing a flat sensitivity in a wide frequency range. These features could make the dual cylinder detector complementary to advanced interferometric detectors, as shown in Fig. 5 by the comparison with the expected sensitivities of LCGT [35] and one of the possible setting of Advanced LIGO in narrow band operation [36].

- 
- [1] S. Kawamura, *Class. Quantum Grav.* **20**, S127 (2003); M. Cerdonio, *ibid.* **20**, S23 (2003).
  - [2] Z.A. Allen *et al.*, *Phys. Rev. Lett.* **85**, 5046 (2000).
  - [3] P. Astone *et al.*, *Phys. Rev. D* **68**, 022001 (2003).
  - [4] D. Sigg, *Class. Quantum Grav.* **19**, 1429 (2002).
  - [5] F. Acernese *et al.*, *Class. Quantum Grav.* **19**, 1421 (2002).
  - [6] See for up to date results: <http://www.ligo.org>
  - [7] J.C. Price, *Phys. Rev. D* **36**, 3555 (1987).
  - [8] C.Z. Zhou and P.F. Michelson, *Phys. Rev. D* **51**, 2517 (1995).
  - [9] S.M. Merkowitz and W.W. Johnson, *Phys. Rev. D* **56**, 7513 (1997).
  - [10] J.A. Lobo, *Mon. Not. R. Astron. Soc.* **316**, 173 (2000).
  - [11] C. Frajuca *et al.*, *Class. Quantum Grav.* **19**, 1961 (2002).
  - [12] E. Coccia, *Class. Quantum Grav.* **20**, S135 (2003).
  - [13] A. de Waard *et al.*, *Class. Quantum Grav.* **20**, S143 (2003).
  - [14] M. Cerdonio *et al.*, *Phys. Rev. Lett.* **87**, 031101 (2001).
  - [15] K. Thorne, in *300 Years of Gravitation*, edited by S. W. Hawking and W. Israel (Cambridge University Press, New York, 1987).
  - [16] T. Briant *et al.*, *Phys. Rev. D* **67**, 102005 (2003).
  - [17] V.B. Braginsky, F.Ya. Khalili, and P.S. Volikov, *Phys. Lett. A* **287**, 31 (2001).
  - [18] A.E.H. Love, *A Treatise on the Mathematical Theory of Elasticity* (Dover, New York, 1944).
  - [19] D.C. Gazis, *J. Acoust. Soc. Am.* **30**, 786 (1958).
  - [20] We assume that the solutions  $\mathbf{u}_e$  and  $\mathbf{u}_i$  are independent.
  - [21] In our approximation this force must be null, with its derivatives, along the  $z$  axis. This condition is fulfilled by the considered GW force and back-action force.

- [22] A. Gillespie and F. Raab, *Phys. Rev. D* **52**, 577 (1995).
- [23] W. Duffy, Jr., *J. Appl. Phys.* **72**, 5628 (1992).
- [24] B. Harnisch *et al.*, *ESA Bull.* **95**, 107 (1998).
- [25] J.P. Zendri *et al.* (unpublished).
- [26] L. Conti, M. De Rosa, and F. Marin, *J. Opt. Soc. Am. B* **20**, 462 (2003).
- [27] A. Marin *et al.*, *Class. Quantum Grav.* **19**, 1991 (2002).
- [28] L. Conti *et al.*, *J. Appl. Phys.* **93**, 3589 (2003).
- [29] R. Mezzena *et al.*, *Rev. Sci. Instrum.* **72**, 3694 (2001).
- [30] S. Kobayashi, *IEEE Trans. Dielectr. Electr. Insul.* **4**, 841 (1997).
- [31] G. Rempe *et al.*, *Opt. Lett.* **17**, 363 (1992).
- [32] F. Marin, L. Conti, and M. De Rosa, *Phys. Lett. A* **309**, 15 (2003).
- [33] H.J. Paik, G.M. Harry, and T. Stevenson, in *Proceedings of the Seven Marcel Grossmann Meeting on General Relativity, Stanford, 1994*, edited by R.T. Jantzen, G. Mac Kreiser, and R. Ruffini (World Scientific, Singapore, 1996), p. 1483.
- [34] S. Kota, *Smart Materials Bulletin*, Vol. 2001 (Elsevier, Amsterdam, 2001), Issue 3, pp. 7–10; J.F. Tressler *et al.*, *IEEE Trans. Ultrason. Ferroelectr. Freq. Control* **45**, 1363 (1998); J. Zhang *et al.*, *Ultrasonics* **37**, 387 (1999).
- [35] K. Kuroda *et al.*, *Class. Quantum Grav.* **19**, 1237 (2002).
- [36] P. Fritschel, *Proc. SPIE* **4856**, 282 (2003).